Published in final edited form as:
*J Am Chem Soc*. 2014 January 22; 136(3): 826–829. doi:10.1021/ja408814g.

# Natural-Like Replication of an Unnatural Base Pair for the Expansion of the Genetic Alphabet and Biotechnology Applications

**Lingjun Li**[†], **Mélissa Degardin**[†], **Thomas Lavergne**[†], **Denis A. Malyshev**[†], **Kirandeep Dhami**[†], **Phillip Ordoukhanian**[‡], and **Floyd E. Romesberg**[†]

Floyd E. Romesberg: floyd@scripps.edu

[†]Department of Chemistry, The Scripps Research Institute, 10550 North Torrey Pines Road, La Jolla, CA, 92037, USA

[‡]Center for Protein and Nucleic Acid Research, The Scripps Research Institute, 10550 North Torrey Pines Road, La Jolla, CA, 92037, USA

## Abstract

We synthesized a panel of unnatural base pairs whose pairing depends on hydrophobic and packing forces and identify d**TPT3**-d**NaM**, which is PCR amplified with a natural base pair-like efficiency and fidelity. In addition, the d**TPT3** scaffold is uniquely tolerant of attaching a propargyl amine linker, resulting in the d**TPT3**$^{\mathbf{PA}}$-d**NaM** pair, which is amplified only slightly less well. The identification of d**TPT3** represents significant progress towards developing an unnatural base pair for the *in vivo* expansion of an organism's genetic alphabet and for a variety of *in vitro* biotechnology applications where it is used to site-specifically label amplified DNA, and it also demonstrates for the first time that hydrophobic and packing forces are sufficient to mediate natural-like replication.

The four letter natural genetic alphabet is conserved throughout nature and is based on the complementary shape and hydrogen-bonding (H-bonding) of the natural nucleotides. Since its original proposal by Benner in 1990,[1] the development of unnatural base pairs has become an active area of research.[2-7] Early efforts focused on novel pairs that form via orthogonal H-bonding patterns, and progress along this route continues.[8] As an alternative approach, inspired in part by Kool's demonstration that H-bonds are not an absolute requirement for replication,[9] our group[2,10-12] and the Hirao group[13-17] have demonstrated that hydrophobic and packing forces are also sufficient to mediate unnatural base pair replication. In particular, we have developed a class of unnatural base pairs, exemplified by d**5SICS**-d**NaM** (Fig. 1A), that when incorporated into DNA are efficiently replicated without sequence bias,[2,18] and efficiently transcribed into RNA.[19,20] However, neither d**5SICS**-d**NaM**, nor any of the other unnatural base pairs reported to date, are replicated with natural base pair-like efficiencies or fidelities. In addition to potentially compromising the potential uses of these unnatural base pairs for both *in vivo* and *in vitro* applications, this raises the fundamental question of whether hydrophobicity and packing forces are truly sufficient to mediate replication with natural-like efficiencies and fidelities.

Correspondence to: Floyd E. Romesberg, floyd@scripps.edu.

Supporting Information. Synthesis, characterization, pre-steady state kinetic data, PCR assay and analysis. This material is available free of charge via the Internet at http://pubs.acs.org.

The d**5SICS**-d**NaM** pair was identified from the optimization of d**SICS**-d**MMO2** (Fig. 1A), which was identified from a screen of 3600 candidate unnatural base pairs.[11] Early optimization efforts focused on improving d**SICS** as a partner for d**MMO2**, eventually yielding d**5SICS**. After progress stalled, our efforts turned to the optimization of d**MMO2** as a partner for d**5SICS**, which eventually yielded d**NaM**.[2,12,18] Although the discovery of d**NaM** represented a significant improvement in replication, continued optimization efforts again stalled,[12,18,21,22,23] implying that further optimization of d**NaM** as a partner for d**5SICS** was unlikely. Thus, our focus turned to the optimization of d**5SICS** as a partner for d**NaM**.

Structural studies in duplex DNA demonstrated that d**5SICS**-d**NaM** forms via cross-strand intercalation.[23,24] This results in a structure that is more similar to a mispair than a correct pair, making the efficient replication of the unnatural base pair difficult to understand. However, recent studies have shown not only that pairing of d**NaM** with d**5SICS**TP within a polymerase active site induces the polymerase to undergo the open-to-closed structural transition characteristic of normal synthesis, but also that within the closed complex, d**NaM** and d**5SICS**TP pair in a Watson-Crick like fashion.[24] This mutually induced fit mechanism is likely responsible for the efficient incorporation of the unnatural triphosphate, but structure-activity relationship (SAR) data suggested that after translocation within the polymerase binding site, in preparation for incorporation of the next triphosphate, the nascent unnatural base pair again returns to an intercalated state, making de-intercalation a requirement for continued DNA synthesis.[12] Thus, we reasoned that further optimization might be possible with d**5SICS** analogs that conform to the SAR rules governing efficient base pair synthesis (via triphosphate incorporation) and extension (via incorporation of the next triphosphate), but that are less prone to intercalate. As SAR data has clearly demonstrated that the thio *N*-glycoside of d**5SICS** is required for both synthesis and extension, we reasoned that modifying and/or reducing the aromatic surface of the second ring might represent a route to favor de-intercalation.

To explore the reduction of aromatic surface area of the d**5SICS** scaffold, as well as to systematically vary nucleobase dipole moment and polarizability, we synthesized the furano and thieno substituted pyridine-2(1H)-thione heterocycles d**FPT1**, d**TPT1**, and d**TPT2** (Fig. 1B, Supporting Information). Briefly, the nucleobase analogs were synthesized via an intermolecular Curtius rearrangement, and then coupled to (2*R*,5*R*)-5-chloro-2-(((4-methylbenzoyl)oxy)methyl) tetrahydrofuran-3-yl 4-methylbenzoate, resulting in a mixture of anomeric nucleosides, with the pure β-anomer obtained by column chromatography. After sulfonylation and toluyl deprotection, the free nucleosides were converted to triphosphates under Ludwig conditions, and purified by anion exchange chromatography and reverse phase HPLC.

In previous work, we employed steady-state kinetics to analyze both unnatural base pair synthesis and extension. However, the chemical steps underlying d**5SICS**-d**NaM** synthesis and extension are sufficiently efficient that under steady-state conditions product formation is limited by dissociation,[25] rendering the steady-state kinetics data less helpful for the optimization of processive replication. Thus, we analyzed the new derivatives using a pre-steady state assay.[22] The assay is based on determining, under a fixed set of conditions, the amount of a 23mer primer that is extended by addition of the unnatural triphosphate opposite its cognate nucleotide in a 45mer template by the Klenow fragment of *E. coli* DNA polymerase I (Kf). The efficiency of unnatural base pair synthesis is characterized by measuring the percent incorporation (%inc) at a given concentration of the unnatural and next correct triphosphate (dCTP), determined from the ratio [24mer+25mer]/[23mer+ 24mer +25mer]. The efficiency of extension is characterized by measuring the percent extension (%ext) at a given concentration of the next correct triphosphate (dCTP) and saturating

concentrations of unnatural triphosphate, determined from the ratio [25mer]/[24mer +25mer]. Under the conditions selected, d**5SICS**TP is incorporated opposite d**NaM** with a %inc of 57, and the resulting d**5SICS**-d**NaM** pair is extended with a %ext of only 15. The derivatives showed a wide range of behaviors (Table 1). d**FPT1**TP is incorporated less efficiently, but d**FPT1**-d**NaM** is then extended more efficiently, while the opposite is true for d**TPT1**TP. However, d**TPT2**TP is incorporated more efficiently than d**5SICS**TP , and the subsequently formed d**TPT2**-d**NaM** pair is also extended more efficiently than d**5SICS**-d**NaM**.

Based on this data we further explored the d**TPT2** scaffold with d**TPT3** (Fig. 1B). With this analog, removal of the methyl group was expected to further modify the tendency of the nucleobase to cross-strand intercalate, and it was synthesized by adaptation of the d**TPT2** synthesis (Supporting Information). Interestingly, both d**TPT3**TP incorporation opposite d**NaM**, and extension of the resulting unnatural pair is more efficient than with d**TPT2**TP (Table 1).

To more fully evaluate replication, the previously reported template D6,[2,26] containing d**5SICS** or a d**5SICS** analog paired opposite d**NaM** was amplified by PCR (in this template, the unnatural base pair is flanked on each side by three randomized natural nucleotides, Supporting Information). Two sets of PCR reactions were explored (Table 1), one employing 48 cycles with OneTaq polymerase, a commercially available mixture of exonuclease-negative Taq polymerase and exonuclease-positive DeepVent polymerases, and one employing 20 cycles of amplification with exonuclease-negative Taq alone, to explore the contribution of proofreading. Efficiency was determined by monitoring amplification level, and fidelity (defined as unnatural base pair retention per doubling) was determined from the percentage of the amplified DNA that retained the unnatural base pair, which was determined from the relative peak intensities of a sequencing chromatogram (Supporting Information and Malyshev, *et al.*[26]). For comparison, with OneTaq natural DNA is amplified $5.5 \times 10^{13}$-fold and DNA containing d**5SICS**-d**NaM** is amplified $9.4 \times 10^{12}$-fold, and 96.3% of the DNA retained the unnatural pair, corresponding to a fidelity of 99.91%. Under these conditions DNA containing d**FPT1**-d**NaM** or d**TPT1**-d**NaM** is amplified $\sim 1 \times 10^{13}$-fold, but with fidelity that is slightly reduced relative to d**5SICS**-d**NaM** (∼98.8%). However, amplification of DNA containing d**TPT2**-d**NaM** proceeded more efficiently than d**5SICS**-d**NaM**, and with an indistinguishable fidelity. Amplification of DNA containing d**TPT3**-d**NaM** again proceeded more efficiently than d**5SICS**-d**NaM**, and remarkably, with no mispaired sequences detected. With a lower limit of detection estimated to be one mispaired sequence in $10^2$ (corresponding to 99% retention), this places a lower limit of 99.98% on the fidelity of d**TPT3**-d**NaM** replication.

Due to the absence of proofreading, amplification with only Taq polymerase is more likely to differentiate the unnatural base pairs. Under the conditions employed with only Taq, natural DNA is amplified $2.8 \times 10^4$-fold and DNA containing d**5SICS**-d**NaM** is amplified $7.7 \times 10^3$-fold and with a fidelity of 98.90%. DNA containing d**FPT1**-d**NaM** or d**TPT1**-d**NaM** is amplified with significantly lower fidelity. However, DNA containing d**TPT2**-d**NaM**, and especially d**TPT3**-d**NaM**, is amplified with greater efficiency and fidelity. In fact, d**TPT3**-d**NaM** is amplified with a fidelity that is only slightly less than that observed with OneTaq. Clearly, based on the pre-steady state kinetics and both PCR conditions, d**TPT2** and especially d**TPT3** are significantly better optimized as partners for d**NaM** than d**5SICS** or any of the other analogs examined.

In principle, an unnatural base pair should allow for the site-specific inclusion of different functionalities into DNA, either pre- or post-amplification,[14,27] for biophysical, *SELEX* (Systematic Evolution of Ligands by Exponential Enrichment)[28,29] or nanomaterial

applications.[30] To explore the potential of the d**TPT3** scaffold for such applications, we synthesized d**FTPT3**TP and d**TPT3$^{PA}$**TP (Fig. 1B), with the former installing an NMR active nuclei for biophysical characterization[31,32] and the latter bearing a linker for the site-specific modification of the amplified DNA. Both analogs were obtained from the toluyl-protected nucleoside of d**TPT3** (Supporting Information). Briefly, d**FTPT3** was obtained in via fluorination, sulfonation, benzoyl deprotection, and phosphorylation, to yield the corresponding triphosphate. d**TPT3$^{PA}$**TP was obtained via iodination, sulfonylation, coupling with the dichloro acetyl propargylamine, deprotection, and phosphorylation.

Both fluoro and propargyl amine substituents have similar effects on the pre-steady state kinetics, slightly reducing the %inc opposite d**NaM**, and more substantially reducing the %ext (Table 1). However, %inc and %ext for both analogs remain significantly greater than those for d**5SICS**. Interestingly, DNA containing either d**FTPT3**-d**NaM** or d**TPT3$^{PA}$**-d**NaM** is PCR amplified with nearly the same fidelity as is d**TPT3**-d**NaM** and remarkably, both are amplified as well or better than DNA containing d**5SICS**-d**NaM** (Table 1). In fact, with Taq alone, d**FTP3**-d**NaM** is better replicated than any previously reported unnatural base pair. The ability of the d**TPT3** scaffold to support the propargyl amine linker is particularly remarkable as d**TPT3$^{PA}$**-d**NaM** is replicated significantly better than d**5SICS$^{PA}$**-d**NaM** (Fig. 1B), which previously was the most efficiently amplified linker-bearing unnatural base pair.[20] With OneTaq, the fidelity is 99.97% versus 98.16% per doubling for d**TPT3$^{PA}$**-d**NaM** and d**5SICS$^{PA}$**-d**NaM**, respectively. Dramatically, with Taq alone, d**5SICS$^{PA}$**-d**NaM** is lost during amplification while d**TPT3$^{PA}$**-d**NaM** is amplified with a fidelity of 98.7%.

Finally, to explore the use of d**TPT3$^{PA}$** for the site-specific labeling of DNA, we examined the amplification, deprotection, and labeling of a 134mer DNA containing a centrally positioned d**TPT3$^{PA}$**-d**NaM** or d**5SICS$^{PA}$**-d**NaM**. Each template was amplified ∼500-fold, deprotected, coupled to NHS-PEG$_4$-biotin, and analyzed by gel shift with streptavidin (Fig. 2A and B). With d**5SICS$^{PA}$**-d**NaM**, 72% of the DNA was shifted, while for d**TPT3$^{PA}$**-d**NaM**, 80% of the DNA was shifted. To explore site-specific labeling at potentially more challenging positions, d**TPT3$^{PA}$**-d**NaM** or d**5SICS$^{PA}$**-d**NaM** was incorporated into a 60mer DNA at the first, ninth, and eleventh position, resulting in duplexes 1–3, respectively (Fig. 2C). With d**5SICS$^{PA}$**-d**NaM**, 6%, 56%, and 84% of the amplified DNA was shifted, while with d**TPT3$^{PA}$**-d**NaM**, 72%, 81%, and 94% was shifted. Clearly, the more efficient amplification of d**TPT3$^{PA}$**-d**NaM**, especially when it is located near the end of a template, results in a significantly greater efficiency of site-specific labeling. This should facilitate many applications, including those requiring that both ends of the same DNA strand are modified, which is otherwise challenging.

In summary, we found that contraction of the distal phenyl ring of d**5SICS** to a methyl thieno ring significantly increases replication, and that subsequent removal of the methyl group increases it still further. These effects are clearly dependent on the detailed structure of the nucleobase. Moreover, it is noteworthy that d**TPT3** represents a rare example among predominantly hydrophobic unnatural base pairs where a reduction in hydrophobicity facilitates replication. A simple explanation for this SAR is that when appropriately positioned, the sulfur atom increases intrastrand packing interactions, while the methyl group favors interstrand packing interactions. Thus, both addition of the sulfur and removal of the methyl group are expected to stabilize the transition state for incorporation, and also favor de-intercalation of the nascent unnatural base pair, which our model predicts would facilitate extension.[12] The robust accommodation of substituents within the d**TPT3** scaffold is also consistent with this model, since only when the pair adopts a Watson-Crick-like structure is a substituent at the position explored predicted to be disposed into the major groove, where it should be relatively non-perturbative.

Regardless of the precise physical underpinnings of its optimized replication, the identification of d**TPT3**-d**NaM** represents a milestone in our effort to expand the genetic alphabet. Under standard PCR conditions, DNA containing d**TPT3**-d**NaM** is amplified by OneTaq with an efficiency that is only 4-fold lower than DNA containing just the natural base pairs, and with a fidelity in excess of 99.98%. This fidelity corresponds to an error rate of $10^{-4}$ per nucleotide, which overlaps with the $10^{-4}$ to $10^{-7}$ error rate of fully natural DNA with commonly used PCR systems.[33] With Taq, the efficiency is only 2.5-fold lower than that of a natural base pair, and the fidelity is 99.7%. This fidelity corresponds to an error rate of $10^{-3}$, which is similar to that observed with the Taq-mediated amplification of natural DNA.[34] This efficient and high fidelity replication should facilitate efforts to expand the genetic alphabet *in vivo* and create the first semisynthetic organism with increased potential for information storage and retrieval. Moreover, the ability of the d**TPT3** scaffold to accommodate a fluoro or protected propargyl amine linker substituent and still be efficiently replicated when paired with d**NaM** suggests that it is a particularly robust scaffold and should make possible a number of *in vitro* applications. Finally, the data demonstrate for the first time that hydrophobic and packing forces are sufficient to mediate the replication of unnatural base pairs with truly naturallike efficiencies and fidelities.

## Supplementary Material

Refer to Web version on PubMed Central for supplementary material.

## Acknowledgments

***Funding Sources***: This work was supported by the NIH (GM 060005).

## References

1. Piccirilli JA, Krauch T, Moroney SE, Benner SA. Nature. 1990; 343:33–37. [PubMed: 1688644]
2. Malyshev DA, Dhami K, Quach HT, Lavergne T, Ordoukhanian P, Torkamani A, Romesberg FE. Proc Natl Acad Sci U S A. 2012; 109:12005–12010. [PubMed: 22773812]
3. Minakawa N, Ogata S, Takahashi M, Matsuda A. J Am Chem Soc. 2009; 131:1644–1645. [PubMed: 19146369]
4. Chelliserrykattil J, Lu H, Lee AH, Kool ET. ChemBioChem. 2008; 9:2976–2980. [PubMed: 19053129]
5. Brotschi C, Mathis G, Leumann CJ. Chem Eur J. 2005; 11:1911–1923. [PubMed: 15685710]
6. Kaul C, Muller M, Wagner M, Schneider S, Carell T. Nat Chem. 2011; 3:794–800. [PubMed: 21941252]
7. Yamashige R, Kimoto M, Takezawa Y, Sato A, Mitsui T, Yokoyama S, Hirao I. Nucleic Acids Res. 2012; 40:2793–2806. [PubMed: 22121213]
8. Yang Z, Chen F, Alvarado JB, Benner SA. J Am Chem Soc. 2011; 133:15105–15112. [PubMed: 21842904]
9. Moran S, Ren RX, Rumney S, Kool ET. J Am Chem Soc. 1997; 119:2056–2057. [PubMed: 20737028]
10. McMinn DL, Ogawa AK, Wu Y, Liu J, Schultz PG, Romesberg FE. J Am Chem Soc. 1999; 121:11585–11586.
11. Leconte AM, Hwang GT, Matsuda S, Capek P, Hari Y, Romesberg FE. J Am Chem Soc. 2008; 130:2336–2343. [PubMed: 18217762]
12. Seo YJ, Hwang GT, Ordoukhanian P, Romesberg FE. J Am Chem Soc. 2009; 131:3246–3252. [PubMed: 19256568]
13. Hirao I. Curr Opin Chem Biol. 2006; 10:622–627. [PubMed: 17035074]
14. Hirao I, Kimoto M, Mitsui T, Fujiwara T, Kawai R, Sato A, Harada Y, Yokoyama S. Nat Methods. 2006; 3:729–735. [PubMed: 16929319]

15. Hirao I, Mitsui T, Kimoto M, Yokoyama S. J Am Chem Soc. 2007; 129:15549–15555. [PubMed: 18027940]
16. Kimoto M, Kawai R, Mitsui T, Yokoyama S, Hirao I. Nucleic Acids Res. 2009; 37:e14. [PubMed: 19073696]
17. Mitsui T, Kitamura A, Kimoto M, To T, Sato A, Hirao I, Yokoyama S. J Am Chem Soc. 2003; 125:5298–5307. [PubMed: 12720441]
18. Lavergne T, Malyshev DA, Romesberg FE. Chem Eur J. 2012; 18:1231–1239. [PubMed: 22190386]
19. Seo YJ, Matsuda S, Romesberg FE. J Am Chem Soc. 2009; 131:5046–5047. [PubMed: 19351201]
20. Seo YJ, Malyshev DA, Lavergne T, Ordoukhanian P, Romesberg FE. J Am Chem Soc. 2011; 133:19878–19888. [PubMed: 21981600]
21. Seo YJ, Romesberg FE. ChemBioChem. 2009; 10:2394–2400. [PubMed: 19722235]
22. Lavergne T, Degardin M, Malyshev DA, Quach HT, Dhami K, Ordoukhanian P, Romesberg FE. J Am Chem Soc. 2013; 135:5408–5419. [PubMed: 23547847]
23. Malyshev DA, Pfaff DA, Ippoliti SI, Hwang GT, Dwyer TJ, Romesberg FE. Chem Eur J. 2010; 16:12650–12659. [PubMed: 20859962]
24. Betz K, Malyshev DA, Lavergne T, Welte W, Diederichs K, Dwyer TJ, Ordoukhanian P, Romesberg FE, Marx A. Nat Chem Biol. 2012; 8:612–614. [PubMed: 22660438]
25. Kuchta RD, Mizrahi V, Benkovic PA, Johnson KA, Benkovic SJ. Biochemistry. 1987; 26:8410–8417. [PubMed: 3327522]
26. Malyshev DA, Seo YJ, Ordoukhanian P, Romesberg FE. J Am Chem Soc. 2009; 131:14620–14621. [PubMed: 19788296]
27. Li Z, Lavergne T, Malyshev DA, Zimmermann J, Adhikary R, Dhami K, Ordoukhanian P, Sun Z, Xiang J, Romesberg FE. Chem Eur J. 2013; 19:14205–14209. [PubMed: 24026962]
28. Keefe AD, Cload ST. Curr Opin Chem Biol. 2008; 12:448–456. [PubMed: 18644461]
29. Kimoto M, Yamashige R, Matsunaga K, Yokoyama S, Hirao I. Nat Biotechnol. 2013; 31:453–457. [PubMed: 23563318]
30. Fritzsche, W.; Bier, F. International Symposium on DNA-Based Nanodevices. American Institute of Physics Conference Proceedings; 2008.
31. Barhate NB, Barhate RN, Cekan P, Drobny G, Sigurdsson ST. Org Lett. 2008; 10:2745–2747. [PubMed: 18533676]
32. Kitevski-LeBlanc JL, Prosser RS. Prog Nucl Magn Reson Spectrosc. 2012; 62:1–33. [PubMed: 22364614]
33. New England Biolabs. PCR Reagents Version 3.0. Ipswich, MA: p. 3
34. Tindall KR, Kunkel TA. Biochemistry. 1988; 27:6008–6013. [PubMed: 2847780]

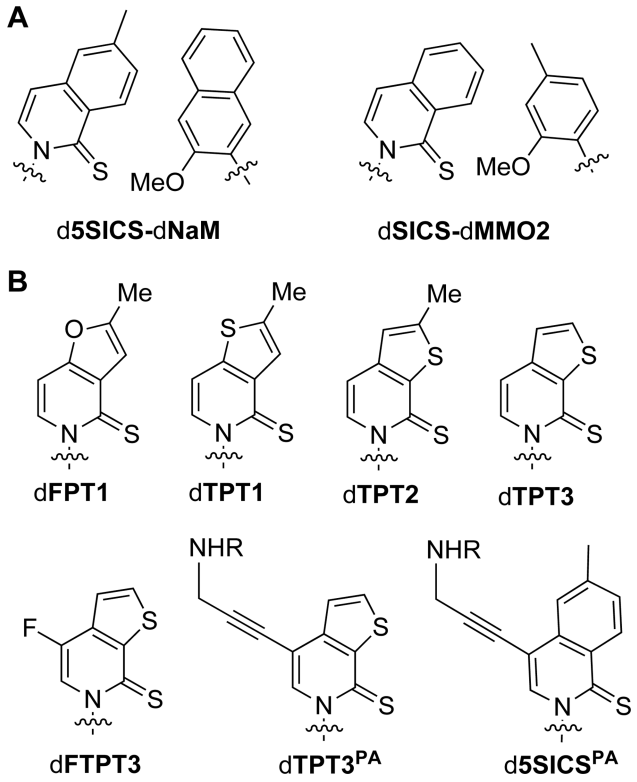


**Figure 1.**
(A) Previously identified unnatural base pairs. (B) Analogs used in this study, with d**5SICS**$^{\mathbf{PA}}$ shown for comparison.[20] R=$COCHCl_2$. Sugar and phosphate backbone are omitted for clarity.

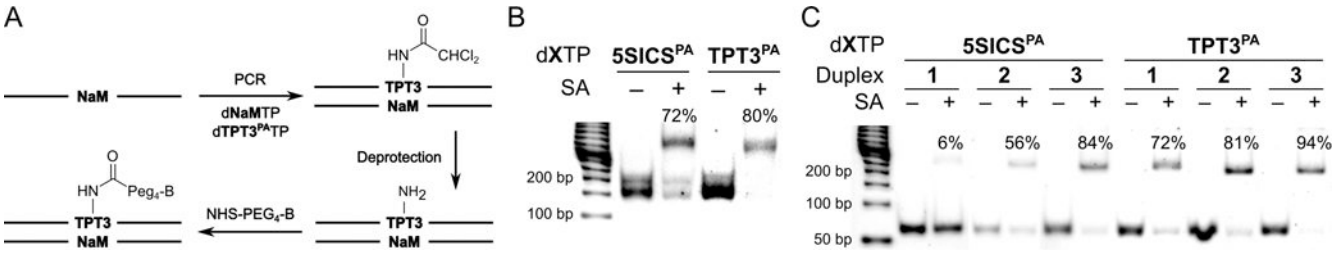


**Figure 2.**

Determination of post-amplification DNA labeling efficiency via streptavidin (SA) gel shift. (A) Labeling strategy (illustrated for d**TPT3**$^{\mathbf{PA}}$-d**NaM**; B = biotin). (B) Labeling with unnatural base pair centrally located in 134mer duplex. The faster and slower migrating bands corresponds to dsDNA, and the 1:1 complex between dsDNA and streptavidin, respectively. (C) Labeling with unnatural base pair positioned at first, ninth, or eleventh positions, corresponding to duplexes 1–3, respectively.

**Table 1**

Kinetic and PCR amplification data.

| | Presteady-state kinetics | | OneTaq PCR (48 cycles) | | | Taq PCR (20 cycles) | | |
|---|---|---|---|---|---|---|---|---|
| **dXTP** | **%inc**[a] | **%ext**[b] | **amplification ×10$^{12}$** | **retention, %** | **fidelity, %** | **amplification ×10$^{3}$** | **retention, %** | **fidelity, %** |
| **5SICS** | 57.0 ± 0.2 | 15.1 ± 1.1 | 9.4 | 96.3 ± 1.7 | 99.91 ± 0.04 | 7.7 | 86.7 ± 1.0 | 98.90 ± 0.01 |
| **FPT1** | 7.2 ± 0.2 | 32.0 ± 1.5 | 9.7 | 62 ± 2 | 98.89 ± 0.09 | 10.9 | 42.0 ± 1.1 | 93.73 ± 0.18 |
| **TPT1** | 28.7 ± 0.5 | 8.8 ± 0.2 | 13.3 | 60 ± 7 | 98.8 ± 0.3 | 6.7 | 33.76 ± 0.03 | 91.81 ± 0.01 |
| **TPT2** | 65.7 ± 0.5 | 34.5 ± 0.5 | 16.6 | 96.8 ± 0.9 | 99.90 ± 0.02 | 9.9 | 93.05 ± 0.04 | 99.46 ± 0.01 |
| **TPT3** | 72.3 ± 0.5 | 49.8 ± 1.3 | 12.9 | > 99 | >99.98 | 11.7 | 95.6 ± 1.7 | 99.66 ± 0.13 |
| **FTPT3** | 66.3 ± 0.5 | 33.8 ± 0.2 | 6.5 | 97.9 ± 1.0 | 99.95 ± 0.02 | 5.0 | 98 ± 3 | 99.9 ± 0.2 |
| **TPT3$^{PA}$** | 68.3 ± 0.4 | 31.5 ± 0.7 | 4.7 | 98.6 ± 1.2 | 99.97 ± 0.03 | 3.5 | 85 ± 4 | 98.7 ± 0.4 |
| **5SICS$^{PA}$** | 7.0 ± 0.2 | 5.5 ± 0.1 | 9.2 | 45 ± 2 | 98.16 ± 0.12 | 6.4 | _[c] | _[c] |

[a] Incorporation assay conditions: 40 nM unnatural triphosphate, 2 μM dCTP, 10 s.

[b] Extension assay conditions: 10 μM unnatural triphsophate, 2 mM dCTP, 10 s.

[c] Unnatural base pair was lost during amplification.

*J Am Chem Soc*. Author manuscript; available in PMC 2015 January 22.